KnE Social Sciences

ISTEcS 2019
Equity, Equality, And Justice In Urban Housing Development
Volume 2019

Knowledge E
enriching | engaging | empowering

Conference Paper

Environmental Quality Assessment of Urban Ecology based on Spatial Heterogeneity and Remote Sensing Imagery

Iswari Nur Hidayati[1], R. Suharyadi[2], and Projo Danoedoro[2]

[1]Doctoral Program, Faculty of Geography, Gadjah Mada University, Indonesia
[2]Departement of Geographic Information Science, Faculty of Geography, Gadjah Mada University, Indonesia

Abstract

The phenomenon of urban ecology is very comprehensive, for example, rapid land-use changes, decrease in vegetation cover, dynamic urban climate, high population density, and lack of urban green space. Temporal resolution and spatial resolution of remote sensing data are fundamental requirements for spatial heterogeneity research. Remote sensing data is very effective and efficient for measuring, mapping, monitoring, and modeling spatial heterogeneity in urban areas. The advantage of remote sensing data is that it can be processed by visual and digital analysis, index transformation, image enhancement, and digital classification. Therefore, various information related to the quality of urban ecology can be processed quickly and accurately. This study integrates urban ecological, environmental data such as vegetation, built-up land, climate, and soil moisture based on spectral image response. The combination of various indices obtained from spatial data, thematic data, and spatial heterogeneity analysis can provide information related to urban ecological status. The results of this study can measure the pressure of environment caused by human activities such as urbanization, vegetation cover and agriculture land decreases, and urban micro-climate phenomenon. Using the same data source indicators, this method is comparable at different spatiotemporal scales and can avoid the variations or errors in weight definitions caused by individual characteristics. Land use changes can be seen from the results of the ecological index. Change is influenced by human behavior in the environment. In 2002, the ecological index illustrated that regions with low ecology still spread. Whereas in 2017, good and bad ecological indices are clustered.

Keywords: spatial heterogeneity, urban ecology, urban remote sensing

Corresponding Author:
Iswari Nur Hidayati
iswari@ugm.ac.id

Received: 24 May 2019
Accepted: 25 July 2019
Published: 4 August 2019

Publishing services provided by Knowledge E

Selection and Peer-review under the responsibility of the ISTEcS 2019 Conference Committee.

1. Introduction

Urban areas are a very complex environment. City also offers a variety of city facilities, transportation, and infrastructure which affects people to move from village to city. Increased urbanization has an impact on urban land change, such as the increase of average air temperature due to the reduced vegetation in urban areas [1]. This

city growth has accelerated the urbanization and industrialization in these regions, leading to dramatic land use and cover change (LUCC) from vegetation to built-up areas. Vegetation cover transformations are so pervasive that when aggregated in a particular place, they significantly impact the key aspects of local ecosystem functioning, such as biodiversity conservation, climate warming, urban heat islands, and water supplies [2]. Therefore it is not easy to solve urban problems quickly, precisely, and accurately. Remote sensing technology is becoming a breakthrough for urban managers to monitor land use change. Remote sensing can be used as a synoptic view for the identification of objects, patterns, and human interactions.

This perspective is particularly useful for researching the urban environment and phenomenon, which can be used for pattern analysis in comfortable city environments [3]. Field measurement is the most commonly used method in urban field research but requires substantial time and cost. Thus remote sensing data is essential for time and cost efficiency. Remote sensing also has a historical perspective in multi-temporal data so that it can be used for the measurement of natural processes in urban, urban growth, urban sprawl, and urban development model. Besides, remote sensing is highly relevant to geo-information technology, such as GIS, spatial analysis, and dynamic modeling, where remote sensing and GIS data can be used for monitoring, synthesizing, and modeling urban environments [4].

Conversion of agricultural land to non-agricultural land and changes in green areas into constructed land are key indicators of land use change. The rapid growth of the built-land results in environmental degradation. Thus, the environmental, ecological impact must be assessed spatially-temporally based on spatial data. Spatial heterogeneity is an unevenly distributed land cover pattern within a region. Spatial heterogeneity patterns are based on spatial dependence variations. Spatial dependence arises when the pixel value in a given location is affected by the pixel value around it. Mixed pixels [5] become quite complicated issues. Several studies have examined issues related to heterogeneity and ecological homogeneity of land surface parameters from remote sensing, e.g., vegetation index, soil surface temperature, soil moisture, built-land, and wetness index.

In remote sensing research, several techniques have been developed to assess spatial and spectral variations. Grid-shaped analyzes of specific pixel sizes that have inter-pixel dependency levels is a challenge in many remote sensing related studies. Spatial dependency in index measurements, such as the Moran Index, is also frequently used in the empirical analysis. However, this index reflects spatial correlation in a general perspective that incorporates all samples, but can not provide information on

homogeneity values in pixels. Measuring local spatial associations, such as semivariance analysis, becomes an alternative to solve the challenge in spatial heterogeneity [6]. Spatial heterogeneity is influenced by the scale, pixel size, and distance on the map so that the type of image used is very influential on the results. Since spatial heterogeneity measurements are dynamic, remote sensing technologies need to be developed to address the spatial heterogeneity problems.

In this study, remote sensing data-based Ecological Index was used to assess spatial-temporal variation in urban ecological changes Yogyakarta over 15 years from 2002-2017. This study aims to monitor the ecological dynamics in urban areas of Yogyakarta in 2002-2017 and identify the static spatial characteristics and dynamic changes in the Ecological Index.

2. Methods and Materials

2.1. Research area

The research area is located in the urban area of Yogyakarta in Province of Daerah Istimewa Yogyakarta (DIY), Indonesia. DIY is astronomically located between 7 ° 33 '-8 ° 12' South Latitude and 110°00'-110 ° 50 'East Longitude (UTM Easting 425773 and UTM northing 9146757). The total area of DIY is 3,185.80 km^2 or 0.17% of the total area of Indonesia (1,860,359.67 km^2). Figure 1 shows Landsat image recorded on September 7, 2017 and August 21, 2002, in the urban area of Yogyakarta.

2.2. Data resources and pre-processing data

Landsat 8 OLI image has 11 bands and 30 m spatial resolution (coastal aerosol, blue, green, red, near infra-red, SWIR 1, SWIR 2, Cirrus), 15 m (panchromatic band) band, 100 m (band infrared thermal 1 and thermal infrared band 2). Landsat 7 ETM + image has blue, green, red, NIR, SWIR 1, SWIR2 (30 m spatial resolution), and thermal bands (60 m spatial resolution). The research processing stages are image pre-processing, image transformation, and image analysis. The Landsat image processing is explained in detail as follows:

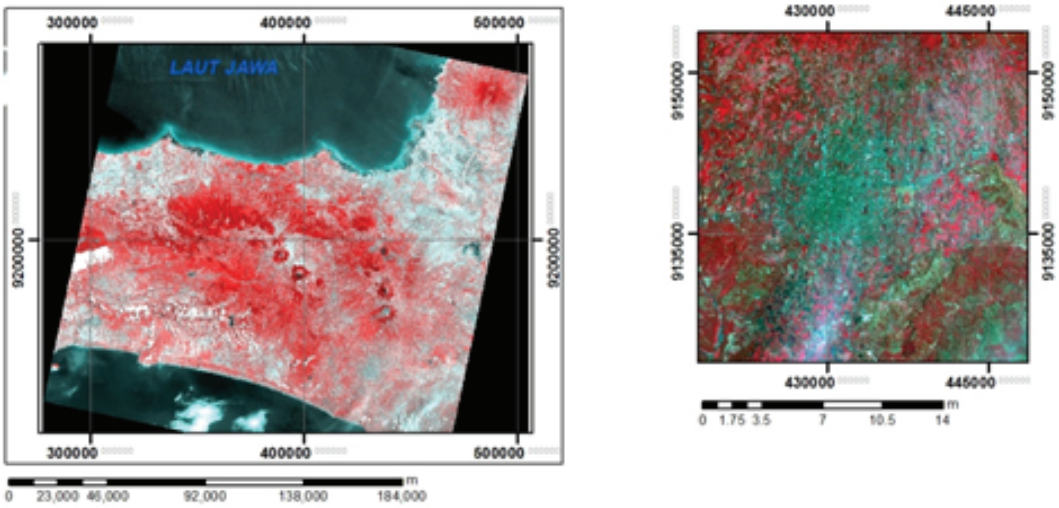

Figure 1: Research Area (Source: Landsat Image, Recording date: 7 September 2017).

2.2.1. Geometric correction

Geometric correction of satellite images involves modeling the relationship between the image and ground coordinate systems. There are both systematic and non-systematic geometric errors in satellite imagery. The systematic errors in Landsat imagery are well documented and are primarily functions of scan skew, mirror-scan velocity, panoramic distortion, platform velocity, perspective and earth rotation [7]. Data of sensor characteristics and ephemeris information are modeled and applied to the raw imagery as part of the systematic correction performed by the Landsat receiving stations. Assuming an accurate correction based on ephemeris model is implemented, systematic errors are corrected in commercially available Landsat imagery (e.g., ACRES Landsat-7 ETM+ Level 5 product). Non-systematic errors are mainly caused by variation through time in the position and attitude angles of the satellite platform. Without accurate parameters of sensor platform orientation, these errors can only be corrected by image-to-map rectification or image-to-image registration using Ground Control Points (GCPs) and a suitable precision photogrammetric or empirical model.

2.2.2. OLI and TIRS at sensor spectral radiance

Images are processed in units of absolute radiance using 32-bit floating-point calculations. These values are then converted to 16-bit integer values in the finished Level-1 product. These values can then be converted to spectral radiance using the radiance scaling factors provided in the metadata file:

$$L_\lambda = M_L * Q_{cal} + A_L \quad (1)$$

where:

L_λ = Spectral radiance (W/(m2 * sr * μm))

M_L = Radiance multiplicative scaling factor for the band (RADIANCE_MULT_BAND_n from the metadata).

A_L = Radiance additive scaling factor for the band (RADIANCE_ADD_BAND_n from the metadata).

Q_{cal} = L1 pixel value in DN

2.2.3. OLI top of atmosphere reflectance

Similar to the conversion to radiance, the 16-bit integer values in the L1 product can also be converted to TOA reflectance. The following equation is used to convert Level-1 DN values to TOA reflectance:

$$\rho\lambda' = M_\rho * Q_{cal} + A_\rho \quad (2)$$

where:

ρ_λ' = TOA Planetary Spectral Reflectance, without correction for the solar angle. (Unitless)

M_ρ = Reflectance multiplicative scaling factor for the band (REFLECTANCE_MULT_BAND_n from the metadata).

A_ρ = Reflectance additive scaling factor for the band (REFLECTANCE_ADD_BAND_n from the metadata).

Q_{cal} = L1 pixel value in DN

Note that ρ_λ' is not true TOA Reflectance, because it does not contain a correction for the solar elevation angle. This correction factor is left out of the L1 scaling at the users' request; some users are content with the scene-center solar elevation angle in the metadata, while others prefer to calculate their own per-pixel solar elevation angle across the entire scene.

2.2.4. Ecological index

The Ecological Index is developed by a combination of three indicators and extracted using Landsat data. The three main indicators in this study are the anthropogenic indicator, environmental indicator, and climate. Land use change is the most prominent process of physical land conversion. Hence, the emphasis on land use change will be represented by the open land index (NDBSI) that reflects the existence of open land and

wake land can be known quickly. The second indicator is the environmental indicator represented by the vegetation index which is NDVI (Normalized Difference Vegetation Index). NDVI is used to detect vegetation against the presence of vegetation. The climate indicator used is LST (Land Surface Temperature) to see changes in temperature and humidity in response to environmental changes.

a. NDBSI (Normalized difference bare land and soil index)

NDBSI considers the index-based built-up index (IBI) used for mapping constructed land. This index looks at the whole in terms of constructed land, bare-land that is not clear of vegetation. IBI is an index that represents the existence of urban land area [8]. The problem of mixed pixels often occurs in urban land-use analysis, requiring other indices to serve open land in urban areas. In this study, we used the Soil Index (SI) [9]. Urban land is made using two indices namely IBI and SI.

b. NDVI (Normalized difference vegetation index)

NDVI (Normalized Difference Vegetation Index) is an image calculation to determine the greenish level, which is very good at the beginning of the division of the vegetation area. NDVI has values ranging from -1.0 to +1.0 [10]. Values greater than 0.1 usually indicate an increase in the degree of greenness and intensity of the vegetation.

c. LSM (Land soil moisture)

LSM is wetness elements in remote sensing imagery used as an indicator in research involving blue, green, red, near infrared, and mid-infrared wavelengths.

d. LST (Land surface temperature)

The standard method for retrieving LST from raw Landsat datasets requires the conversion of the DN values of the thermal bands (Band 6 in Landsat ETM+, and Bands 10 and 11 in Landsat TIRS) into at-satellite spectral radiance values (Lλ) [11]. And then into the at-satellite brightness temperature (Tb), which is calculated under an assumption of unity emissivity (ε) and using pre-launch calibration constants [12]. A correction for spectral emissivity follows this process according to the nature of the landscape. In this study, we used the thermal Band 6 of Landsat ETM + and Band 10 of Landsat OLI to

retrieve the LST for the years 2000 and 2016, respectively. The calculations of Lλ, Tb, ε, and LST were performed in light of these references[13].

e. Data resources and pre-processing data

The creation of the Ecological Index uses the principal component analysis (PCA) to combine the three indices. PCA is a mapping procedure used to summarize several bands into fewer bands. Rodarmel & Shan (2002) [14] mentioned that the correlation matrix in PCA is more suitable for measuring different units when compared to covariance matrices. The complexity parameter also influences high accuracy in PCA. The degree of correlation of the parameters depends on the scale mapping.

Consequently, the aggregation rate of the pixel can produce components better than others when adapted to the synergism between parameters and influenced by spatial resolution. The PCA is based on the correlation matrix that alters the variables measured at different scales to obtain the chosen standard value. This PCA will provide several methods of combining spatial data and spectral data. Matrix correlation analysis is performed to find out the relationship between two or more data. If the variables change then, the changes must be related to other variables. The perfect linear correlation with few frequencies can be found in the PCA processing. However, these results are rare in the PCA process. The ecological index formed from 3 indices will result in three different PCA bands with different results. If the value is represented by one of the main components (PC1), then the value formed is the single integrated index value. The degree of truth in correlation analysis depends on the parameters and scale (modifiable area unit problem). Thus, one level of pixel data aggregation can result in higher component loads when compared to others. This is adapted to the synergism between the parameters of each scale.

2.3. Spatial heterogeneity analysis

The analysis focused on clustering aspects, which the name of spatial clustering and ecological index. Moran's I is a correlation coefficient that measures the overall spatial autocorrelation [2]. In other words, it measures how one object is similar to others surrounding it. If objects are attracted (or repelled) by each other, it means that the observations are not independent. This violates a basic assumption of statistics-independence of data. In other words, the presence of autocorrelation renders most statistical tests invalid, so it is important to test for it. Moran's I is one way to test for autocorrelation.

Spatial autocorrelation is multi-directional and multi-dimensional, making it useful for finding patterns in complex data sets. It is similar to correlation coefficients. It has a value from -1 to 1. However, while other coefficients measure perfect correlation to no correlation, Moran's is slightly different (due to the more complicated, spatial calculations). -1 is perfect clustering of dissimilar values (you can also think of this as perfect dispersion). 0 is no autocorrelation (perfect randomness.), and +1 indicates perfect clustering of similar values (it is the opposite of dispersion). The Moran index cannot indicate the hot spots in this study [16]

2.4. Semi-variance analysis

Semi-variance is used for geospatial calculations associated with spatial continuity in Ecological Index values. The value of the experimental semivariance for a vector is derived from calculating one-half the average squared difference between every data pair separated by a specific lag distance of *h* [6]

3. Result and Discussion

3.1. Data analysis result

Vegetation provides a spectral response at visible wavelengths with lots of absorbed energy and less transmitted energy. Wavelength in the range 0.54 µm-0.50 µm is the green spectrum is the chlorophyll absorption area, resulting in a high enough reflection, while in the near infrared spectra, green vegetation provides a very high reflection [17]. Hoffer & Johannsen (1969) [18] also mentioned that in the near-infrared spectrum, healthy green leaves tend to reflect more and continue electromagnetic forces, but absorb less electromagnetic energy. This tendency leads to near-infrared spectra very sensitive to changes in leaf density levels, as part of the infrared spectrum power will be re-reflected by the leaf surface below. In the green band, the spectral reflectance value of vegetation will be good. The red, green, and blue channel combinations produce a true color composite. Other channel combinations produce a false-color composite (Fig.2) The spectral reflection of vegetation is influenced by the number and extent of the leaves. The vegetation index is a combination of several bands that can produce information related to vegetation density. Houborg et al., (2011) [19] stated that the phenomenon of red-light absorption by chlorophyll (0.4 µm - 0.7 µm) in vegetation and infrared light

reflections close to mesophyll tissue (0.7 µm - 1.1 µm) in the leaves will make differences in brightness values.

Pettorelli et al., (2005) also researched by testing various bands such as near-infrared, red bands, and green bands to predict biomass contents, and chlorophyll content on the grass. Normalized Difference Vegetation Index (NDVI) is chosen because the comparison form between infrared bands close to the red band will minimize the irradiance conditions caused by changes in sun angle, topography, atmospheric conditions, and cloud cover. Jawak & Luis (2013) [20] found that the NDVI values obtained by high-resolution images still have a high correlation and the spectral characteristics are unchanged when NDVI is applied at high spatial resolution. Other studies suggest that the NDVI profile in high-resolution images is very similar to NDVI processing in the original multispectral image value, so there is no significant change when using high-resolution images as well as the medium resolution in NDVI processing [21]. The result of NDVI transformation is given in Fig 3. It was found that NDVI value from Landsat Image in 2002 had a minimum value of -0.65 and a maximum value of 0.002. The value of the threshold used to distinguish the vegetation area and not vegetation area is -0.32. This means that the vegetated area is not always more than 0. The spectral reflection of the image will affect the results of the threshold processing. NDVI in 2017 had minimum value -0.51 and the maximum value of index 0.05. The standard deviation in 2002 was 0.10 and in 2017 was 0.08. The threshold value used to differentiate the vegetation and non-vegetation areas was -0.32

(a) Landsat 2002, 742 band combination (b) Landsat 2017, 742 band combination

Figure 2: Landsat Imagery False Color Composite.

The urban surface is more complicated phenomena, and spectral heterogeneity in this area is notable due to the spatial resolution, especially for a thermal image. So the occurrence of a mixed pixel is collective and therefore effective emissivity should be considered more cautiously. Land soil moisture conditions play a critical role in evaluating terrestrial environmental conditions related to ecological, hydrological, and

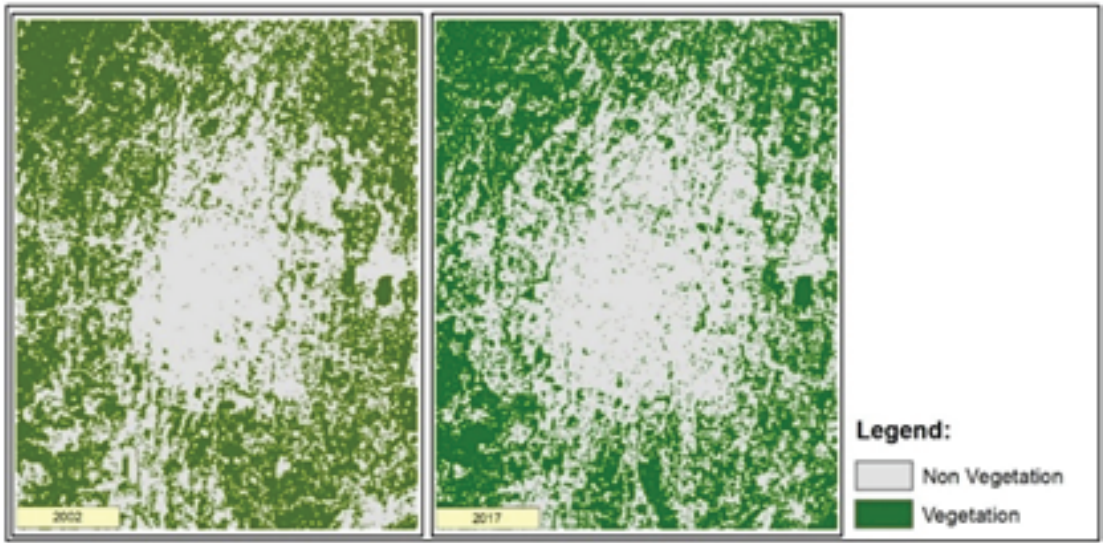

Figure 3: Transformation of NDVI.

atmospheric processes. Extensive efforts to exploit the potential of remotely sensed observations to help quantify this complex variable are still underway. From the result of image processing in 2002, it was obtained the value of LSM was minimal -0.83 and maximum 0.04, with Standard deviation 0.045. The soil moisture index value generated from 2017 had a maximum value of -0.29 and a standard deviation of 0.06 (Fig 5). The threshold value of -0.16 was used to divide between an area that has high and low humidity. This means that areas with pixel values below -0.16 are areas with low humidity and areas with values above -0.16 are areas that have high humidity which also have a positive correlation to vegetation.

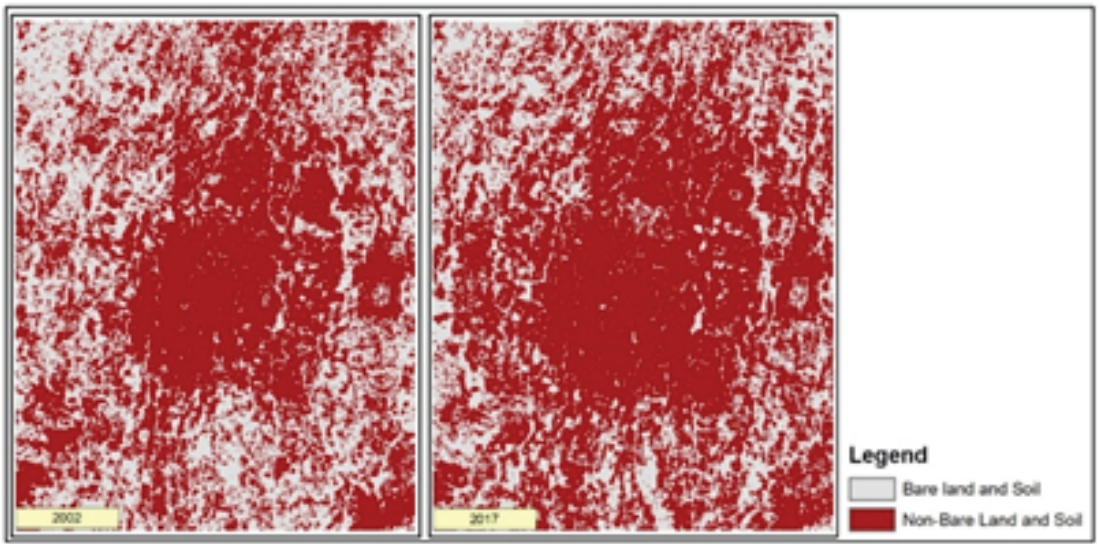

Figure 4: Normalized Difference Bare-land Index and Soil Index.

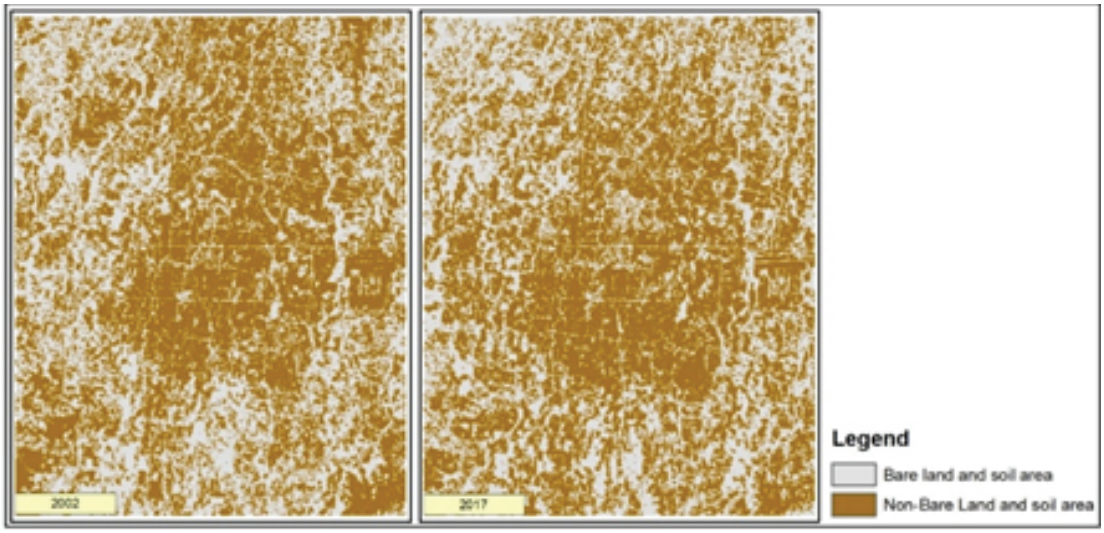

Figure 5: Land Surface Moisture.

Land surface temperature (LST) is an important factor for the determination of several biophysical parameters and processes. Increasing urbanization and industrialization has caused changes in the heat balance densely built urban areas. In such cases, LST is usually higher than the temperatures of the surroundings. Surface temperature is known by calculating LST value. This LST represents weather and moisture elements. The results of image processing in 2002 showed that the lowest temperature was 21°C and the highest temperature was 44°C. While the image processing results in 2017 showed the lowest temperature was 24.34 °C, and the highest temperature was 36.89°C. From these results, the increased temperature in the urban area of Yogyakarta was 3°C.

3.2. Ecological index

These statistics provide a single value that describes the spatial autocorrelation of the dataset as a whole. ENVI Classic offers three global spatial statistics, consisting of the spatial autocorrelation statistics known as Moran's I, Geary's C, and semivariance. The Moran's I index compares the differences between neighboring pixels and the mean to provide a measure of local homogeneity. The value range is between +1 and -1, where +1 = strong positive spatial autocorrelation, 0 = spatially uncorrelated data, and -1 = strong negative spatial autocorrelation. The Geary's C index compares the differences between neighboring pixels to the standard deviation to provide a measure of dissimilarity within a dataset. The value range is between 0 and 2, where 0 = strong positive spatial autocorrelation, 1 = spatially uncorrelated data, and 2 = strong negative spatial autocorrelation. The semivariance statistic uses the squared difference between

neighboring pixel values to provide another measure of dissimilarity within a dataset. It differs from the unit less Moran's I and Geary's C indices in that it is in the same units of the input dataset, and the value range is only constrained to be greater than or equal to 0. While autocorrelation statistics indicate the local homogeneity of a dataset, it is sometimes interesting to understand how that autocorrelation decreases as distance increases. In statistics, the standard deviation is a measure used to measure the amount of variation or distribution of a certain amount of data values. The lower the standard deviation, the closer to the average, whereas if the standard deviation value is higher than the width of the range of data variations, then the standard deviation has a big difference from the sample value to the average.

Based on the research result of the making of Ecological Index, it was calculated that standard deviation value for the year 2002 was 0.81 and for the year of 2007 was 0, 82 (Fig.7). This means that the data range from 2002 to 2017 is quite high. The Moran Index (Moran's I) is the most widely used method for calculating global spatial autocorrelation. This method can be used to detect the beginnings of spatial randomness. The range of values of the Moran Index in the case of the standardized spatial weighted matrix is $-1 \leq I \leq 1$. The value $-1 \leq I < 0$ indicates the existence of spatial autocorrelation negative, while the value $0 < I \leq 1$ indicates a positive spatial autocorrelation, the value of the zero Moran Index indicates non-grouping. The Moran Index value does not guarantee the accuracy of the measurement if the weighting matrix used is weighted un-standardized. The Moran Index of the study was 0.78 and 0.79. From these results, it can be seen that the differences between adjacent pixels have a reasonably high correlation and reflect the spatial homogeneity. The ecological appearance in the research area is quite homogeneous in urban built-up land. Fig. 7 indicated that the values of Moran's I and R2 in the spatial autocorrelation analysis monotonically decreased with the increase in the grain size.

The values of the sill, the ratio, and the range all decreased from 2002 to 2017 (Table 2), which indicated that there were a lower spatial autocorrelation and higher spatial heterogeneity percentage in the ecological index in 2017 than in 2002 (Fig. 8). This trend indicates that urban sprawl development has a significant effect on the spatial structure of the eco-environment as measured by the ecological index. This finding shows that the results of these two methods (i.e., spatial autocorrelation analysis and semivariance analysis) are consistent, and only the combination of these two methods can better explain the spatial paradigm of the observation. The calculation of the trial semivariance considering all the pixels in all directions within the entire study area is the most difficult method and a very time-consuming process due to a large number

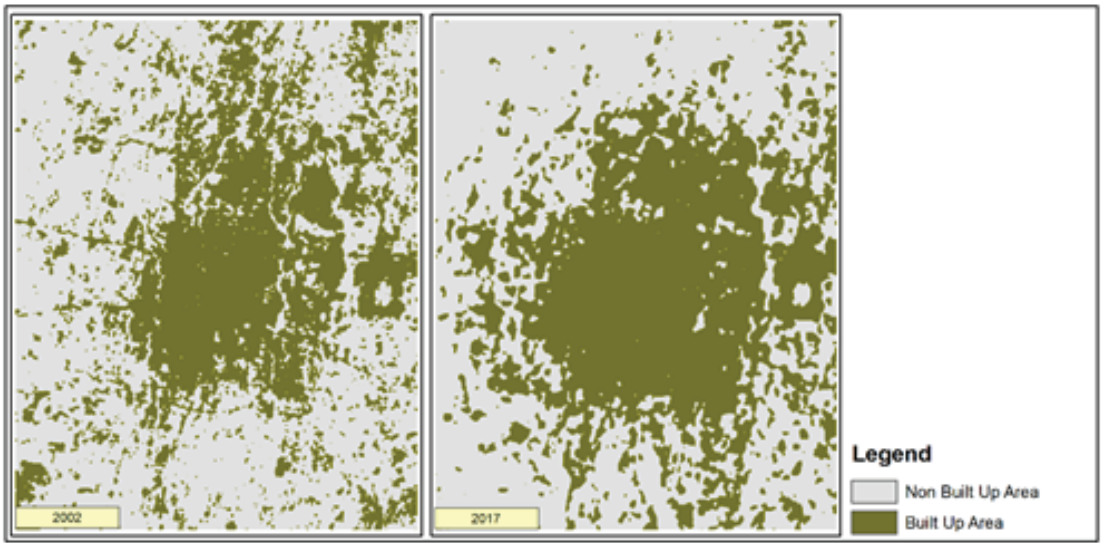

Figure 6: Land Surface Temperature.

of explanations involved in the calculation. This conclusion is constant with this study that used an urban area as the observation object, in which populations and buildings were highly concentrated. In general, the eco-environment was more deficient in the central section than it was in the peripheral areas close to the rural zone. A notable characteristic of the distribution in Ecological Index was that the environmentally weak areas were gathered in the center in 2017, while it was more dispersed in 2002.

TABLE 1: Description Statistic of Ecological Index.

Year	Min	Max	SD	Autocorrelation Moran Index	Autocorrelation Index (Geary's C)	Semi variance
2002	-1.09	0.9	0.81	0.79	0.20	0.13
2017	-0.97	1.0	0.82	0.78	0.21	0.14

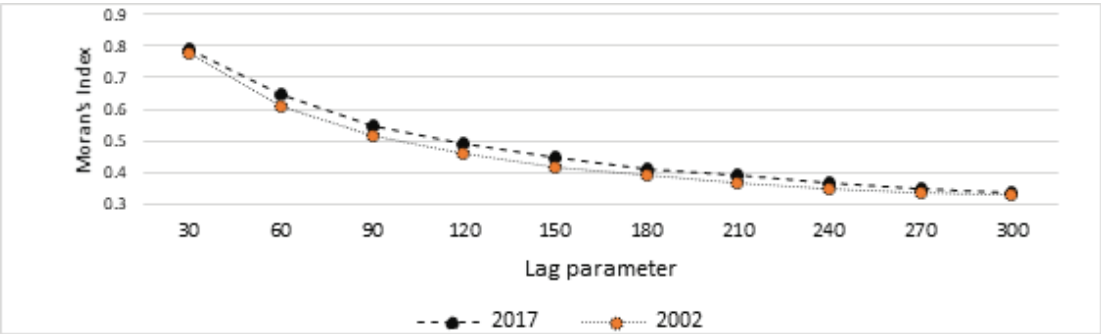

Figure 7: Parameters of spatial autocorrelation respond to grain sizes in years between 2002 and 2017.

The Ecological Index in this study is a combination of soil moisture index, vegetation index, and index of built land and equipped with surface temperature. This Ecological Index will respond to the ecosystem from the pressure, status, and response to the

ecosystem itself. The index is made using PC1 derived from four main factors: human (illustrated by building index), environmental changes represented by vegetation index, climate change (temperature and humidity, LST). This Ecological Index can be seen and compared using different temporal-spatial measures considering spatial homogenates and spatial heterogeneity. From the results of the index, processing can be seen that the decline of both the vegetation area from 2002-2016. Analysis of semivariance and autocorrelation showed that spatial correlation in the Ecological Index distribution has the highest value outside the city and the lowest value in the city. The results of the semivariogram analysis show that high levels of human interference in the study area lead to significant environmental degradation and land use change. The analysis of the spatial autocorrelation and semivariance indicated that there was a spatial correlation in the distribution of the ecology index, with the high value in the edge and the low value in the center of the city. The values of the sill, the nugget/sill ratio, and the range all increased from 2002 to 2017. Based on the combination with the spatial clusters and the spatiotemporal clusters, we confirmed that the Ecological Index is not randomly distributed. Moreover, a hole-effect semivariogram was observed, indicating a high level of human intervention in the study area. Specifically, the construction of the built-up area during the study period led to ecological degradation outward, and urban afforestation promoted good environmental quality in the central urban area.

3.3. Conclusion

This combination of indices is one of the innovations for assessing the Ecological Index. This index helps to understand the complexity of pressure variations and environmental responses to ecosystems. The Ecology Index was built using PC1 from the three factors: urbanization (building index), vegetation coverage, and climate change responses. This index can eliminate variations caused by individual characteristics and be used in various scales and. We concluded that human activities influence changes in the ecological index. In using the advantage of having the same data source for all the indicators, the ecological index was found to be scalable and comparable at different spatiotemporal scales and can avoid the variation or error in weight definitions caused by individual characteristics. The results showed that the Yogyakarta urban area practiced ecological deterioration through the study period from 2002 to 2017, with the ecological Index value increasing from 0.81in 2002 to 0.82 in 2017. A set of parameters was then extracted from the autocorrelation and semi-variance analysis to measure the heterogeneity of the spatial distribution in the Index. Specifically, the structure of the built-up area during

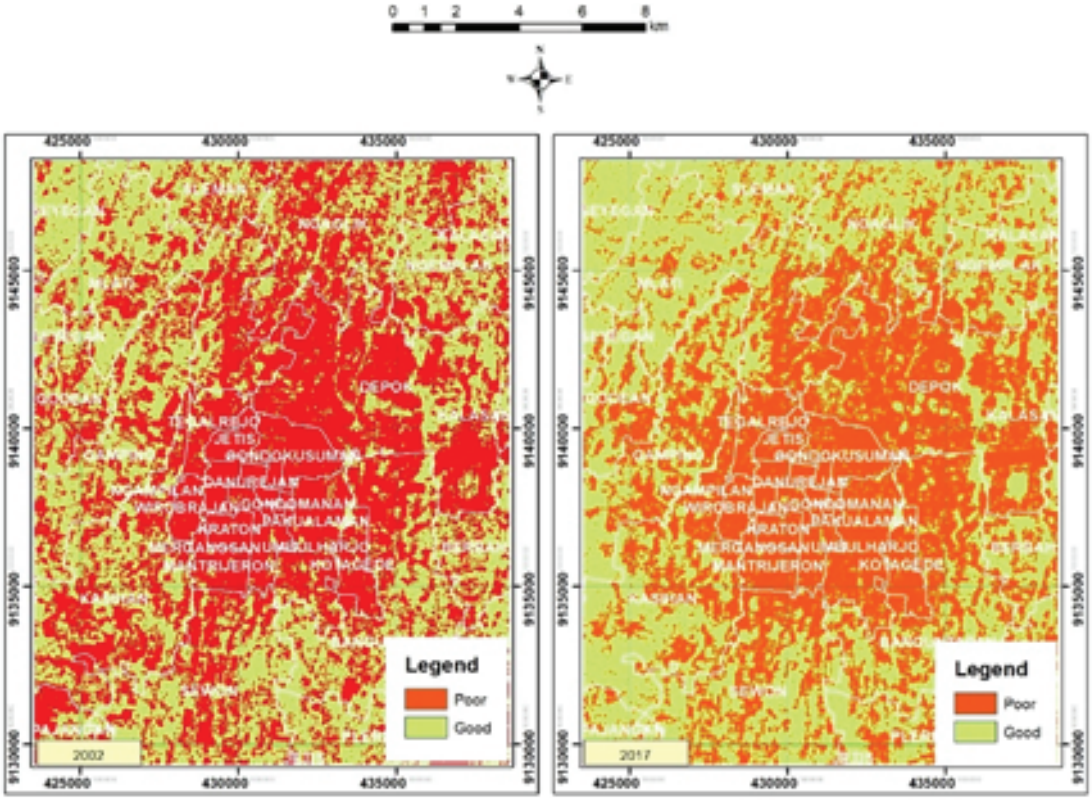

Figure 8: Spatial Distribution of Ecological Index in Yogyakarta Urban Area.

the study period led to ecological degradation outward. Finally, this index can be used efficiently and effectively to see changes in land use, and it's affecting factors.

References

[1] Weng, Q., & Fu, P. (2014). Modeling annual parameters of clear-sky land surface temperature variations and evaluating the impact of cloud cover using time series of Landsat TIR data. *Remote Sensing of Environment*, *140*, 267-278

[2] Fuglsang, M., Münier, B., & Hansen, H. S. (2013). Modelling land-use effects of future urbanization using cellular automata: An Eastern Danish case. *Environmental modelling & software*, *50*, 1-11.

[3] Zhang, X., Estoque, R. C., & Murayama, Y. (2017). An urban heat island study in Nanchang City, China based on land surface temperature and social-ecological variables. *Sustainable cities and society*, *32*, 557-568..

[4] Pettorelli, N., Vik, J. O., Mysterud, A., Gaillard, J. M., Tucker, C. J., & Stenseth, N. C. (2005). Using the satellite-derived NDVI to assess ecological responses to environmental change. *Trends in ecology & evolution*, *20*(9), 503-510.

[5] Aubrecht, C., Steinnocher, K., Hollaus, M., & Wagner, W. (2009). Integrating earth observation and GIScience for high resolution spatial and functional modeling of urban land use. *Computers, Environment and Urban Systems*, *33*(1), 15-25.

[6] Nwogugu, M. (2007). *Correlation, covariance, variance and semi-variance are irrelevant in risk analysis, portfolio management and mechanics*. Working paper). Available at www. ssrn. com.

[7] Sindeaux, R., de Souza Figueiredo, P. T., de Melo, N. S., Guimarães, A. T. B., Lazarte, L., Pereira, F. B.,... & Leite, A. F. (2014). Fractal dimension and mandibular cortical width in normal and osteoporotic men and women. *Maturitas*, *77*(2), 142-148.

[8] Gangulya, K., & Shankar, G. R. (2014). Geo-environmental appraisal for studying urban environment and its associated biophysical parameters using remote sensing and GIS technique. *International Archives of the Photogrammetry, Remote Sensing and Spatial Information Sciences*, *8*.

[9] Huete, A. R. (1988). A soil-adjusted vegetation index (SAVI). *Remote sensing of environment*, *25*(3), 295-309.

[10] Prabhakara, K., Hively, W. D., & McCarty, G. W. (2015). Evaluating the relationship between biomass, percent groundcover and remote sensing indices across six winter cover crop fields in Maryland, United States. *International journal of applied earth observation and geoinformation*, *39*, 88-102.

[11] Sharma, R., Ghosh, A., & Joshi, P. K. (2013). Spatio-temporal footprints of urbanisation in Surat, the Diamond City of India (1990–2009). *Environmental monitoring and assessment*, *185*(4), 3313-3325.

[12] Xu, W., Wooster, M. J., & Grimmond, C. S. B. (2008). Modelling of urban sensible heat flux at multiple spatial scales: A demonstration using airborne hyperspectral imagery of Shanghai and a temperature–emissivity separation approach. *Remote Sensing of Environment*, *112*(9), 3493-3510.

[13] Al-Hamdan, M., Quattrochi, D., Bounoua, L., Lachir, A., & Zhang, P. (2016). Using Landsat, MODIS, and a Biophysical Model to Evaluate LST in Urban Centers. *Remote Sensing*, *8*(11), 952.

[14] Rodarmel, C., & Shan, J. (2002). Principal component analysis for hyperspectral image classification. *Surveying and Land Information Science*, *62*(2), 115-122.

[15] Barbosa, D. S., Belo, V. S., Rangel, M. E. S., & Werneck, G. L. (2014). Spatial analysis for identification of priority areas for surveillance and control in a visceral leishmaniasis endemic area in Brazil. *Acta Tropica*, *131*, 56-62.

[16] Lanorte, A., Danese, M., Lasaponara, R., & Murgante, B. (2013). Multiscale mapping of burn area and severity using multisensor satellite data and spatial

autocorrelation analysis. *International Journal of Applied Earth Observation and Geoinformation*, *20*, 42-51.

[17] Roy, D. P., Wulder, M. A., Loveland, T. R., Woodcock, C. E., Allen, R. G., Anderson, M. C.,... & Scambos, T. A. (2014). Landsat-8: Science and product vision for terrestrial global change research. *Remote sensing of Environment*, *145*, 154-172.

[18] Hoffer, R. M., & Johannsen, C. J. (1969). Ecological potentials in spectral signature analysis. *Remote sensing in ecology*, 1-16.

[19] Houborg, R., Anderson, M. C., Daughtry, C. S. T., Kustas, W. P., & Rodell, M. (2011). Using leaf chlorophyll to parameterize light-use-efficiency within a thermal-based carbon, water and energy exchange model. *Remote Sensing of Environment*, *115*(7), 1694-1705.

[20] Jawak, S. D., & Luis, A. J. (2013). A spectral index ratio-based Antarctic land-cover mapping using hyperspatial 8-band WorldView-2 imagery. *Polar Science*, *7*(1), 18-38.

[21] Amani, M., Salehi, B., Mahdavi, S., Masjedi, A., & Dehnavi, S. (2017). Temperature-vegetation-soil moisture dryness index (tvmdi). *Remote sensing of environment*, *197*, 1-14.